arXiv:1403.7250v1 [math-ph] 27 Mar 2014

On the Spectral Domain of Large Nonsymmetric Wishart Correlation Matrices

Vinayak[1,*] and Luis Benet[1,†]

[1] *Instituto de Ciencias Físicas, Universidad Nacional Autónoma de México, C.P. 62210 Cuernavaca, México*

We study the complex eigenvalues of the Wishart model defined for nonsymmetric correlation matrices. The model is defined for two statistically equivalent but different Gaussian real matrices, as $\mathsf{C} = \mathsf{A}\mathsf{B}^t/T$, where B^t is the transpose of B and both matrices A and B are of dimension $N \times T$. We consider *actual* correlations between the matrices so that on the ensemble average C does not vanish. We derive a loop equation for the spectral density of C in the large N and T limit where the ratio N/T is finite. The actual correlations changes the complex eigenvalues of C, and hence their domain from the results known for the vanishing C or for the uncorrelated A and B. Using the loop equation we derive a result for the contour describing the domain of the bulk of the eigenvalues of C. If the nonvanishing-correlation matrix is diagonal with the same element $c \neq 0$, the contour is no longer a circle centered at origin but a shifted ellipse. In this case, the loop equation is analytically solvable and we explicitly derive a result for the spectral density. For more general cases, our analytical result implies that the contour depends on its symmetric and anti-symmetric parts if the nonvanishing-correlation matrix is nonsymmetric. On the other hand, if it is symmetric then the contour depends only on the spectrum of the correlation matrix. We also provide numerics to justify our analytics.

PACS numbers: 02.50.Sk, 05.45.Tp, 89.90.+n

I. INTRODUCTION

Correlation matrices are fundamental in multivariate analysis [1–3]. Examples thereof are not only in econophyscis [4–8] but also in biological sciences [9, 10] and atmospheric science [11] among others. In such studies, often random matrix theory (RMT) proved to be remarkably useful. The basic random matrix model for the correlation matrices is due to Wishart [3], which is often being credited as the origin of RMT [12]. The situation dealt in this model is quite generic [1–3], viz., the model refers to a multivariate system where all the time series are stochastic with all statistically independent variables. Notably, beyond the conventional theme, potential of this model has been realized in physics [12–15] and in communication engineering [16] as well.

In multivariate analysis, estimation of the *actual* correlation matrix is difficult due to the finiteness of the time horizon which results noise in the empirical correlation matrix. The Wishart model provides a framework against which the actual correlations must be viewed. For instance, the famous Marčenko-Pastur formula [17] has been remarkably useful [4–7, 9–11, 18] in identifying bulk and collective properties of diverse statistical systems. Nevertheless, a simple generalization by including linear correlations in this model improves the the so-called *null hypothesis* [18] and provides a better platform to understand the underlying correlations [19–26]. These models are often referred to as the correlated Wishart orthogonal ensembles (CWOE). These models go beyond the basic model, letting the averaged correlation matrix not to be simply proportional to an identity matrix. Recent interests in these studies have been the nonsymmetric correlation matrices [27–33] where plenty of results are known for the uncorrelated case. Motivations behind the nonsymmetric correlation matrices are twofold: The nonsymmetry is natural for a correlation matrix describing statistics between two different statistical systems while the time-lagged correlation matrix is also nonsymmetric. The latter is interesting from the viewpoint of forecasting models. The corresponding Wishart model for nonsymmetric correlation matrices is defined via two statistically equivalent but different Gaussian real matrices A and B, as $\mathsf{C} = \mathsf{A}\mathsf{B}^t/T$ where the entries of each of the matrices are real Gaussian variables with 0 mean and variance 1. For the uncorrelated case, where C vanishes on average, the density of the singular values was derived in Refs. [29, 34, 38–40]. Using the CWOE approach, this result has been generalized for large matrix dimensions for the nonvanishing C [33].

The matrix which defines the time-lagged correlations for a system of conserved number of variables is square and thus has complex eigenvalues which again have been useful in analyzing the financial data [28, 32]. In these studies, the analytical results used are derived for the case where on average C vanishes [34–37]. In this paper, we use the same approach as described in [33] and derive results for the nonvanishing C. In particular, we consider $\overline{\mathsf{A}\mathsf{B}^t}/T = \eta$, where the overbar denotes ensemble averaging, and η is the $N \times N$ correlation matrix which defines the *actual correlations*. The joint probability density of the matrix elements of A and B can be described via

$$P(\mathsf{A},\mathsf{B}) \propto \exp\left[-\frac{T}{2}\mathrm{tr}\left\{\begin{pmatrix}\mathbf{1}_N & \eta\\ \eta^t & \mathbf{1}_N\end{pmatrix}^{-1}\begin{pmatrix}\mathsf{A}\\ \mathsf{B}\end{pmatrix}\left(\mathsf{A}^t\,\mathsf{B}^t\right)\right\}\right], \tag{1}$$

where matrices A and B both are of dimension $N \times T$ and

*Electronic address: vinayaksps2003@gmail.com
†Electronic address: benet@fis.unam.mx

for an integer K, $\mathbf{1}_K$ is an identity matrix of dimensions $K \times K$. Using the techniques developed in Refs. [41–45], and used recently for the $\eta = 0$ case in Ref. [34], in this paper we derive the loop equations for the spectral density of C at large matrix dimension. We solve these equation and obtain a formula for the contour describing the boundary of the bulk of eigenvalues of C. Interestingly, for the symmetric η, the contour depends only on the spectrum while for nonsymmetric η it depends on the symmetric and the anti-symmetric part of η. We present some examples for the tridiagonal η to demonstrate the results. Moreover, we derive the spectral density for two cases, viz., (i) $\eta_{jk} = c$ and (ii) $\eta_{jk} = c\,\delta_{jk}$. We show that in both cases the density depends only on the radial distance; however, in the latter case the contour is no longer a circle centered at origin but a shifted ellipse.

In the next section we define the nonsymmetric correlation matrices from the CWOE approach, fix the notation and describe some generalities for the analytics. In Sec. III, we derive the loop equation. In section IV, we derive the formula for the contours defining boundaries of the bulk of complex eigenvalues for the η's for which the full correlation matrix is positive definite. In Sec. V, we compare our analytics with numerics for tridiagonal η. In Sec. VI, we solve the loop equation for some especial cases, as discussed above. In Sec. VII, we give a summary of the work with conclusions.

II. GENERALITIES

The problem we address in this paper is closely related to CWOE. CWOE is an ensemble of real symmetric matrices of type $\mathcal{C} = \mathcal{W}\mathcal{W}^t/T$. For CWOE, $\mathcal{W} = \xi^{1/2}\mathcal{W}'$ where ξ is a real symmetric positive definite nonrandom (fixed) matrix and the entries of the matrix $\mathcal{W}'$ are independent real Gaussian variables with mean 0 and variance 1. Thus, on average we have

$$\overline{\mathcal{C}} = \xi. \tag{2}$$

In our case the matrix $\mathcal{W}$ constitutes of two different random matrices A and B, as

$$\mathcal{W} = \begin{pmatrix} \mathsf{A} \\ \mathsf{B} \end{pmatrix}, \tag{3}$$

where A and B are both of dimensions $N \times T$. The ensemble correlation matrix ξ we consider here is given by

$$\xi = \begin{pmatrix} \mathbf{1}_N & \eta \\ \eta^t & \mathbf{1}_N \end{pmatrix}, \tag{4}$$

where the diagonal blocks imply only self-correlations among the variables of A and B. The off-diagonal η-blocks accounts for the correlations between A and B. The correlation matrix we are interested in corresponds to the upper off-diagonal block of $\mathcal{C}$:

$$\mathsf{C} = \frac{1}{T}\mathsf{A}\mathsf{B}^t, \tag{5}$$

so that $\overline{\mathsf{C}} = \eta$. Here we also define the ratio,

$$\kappa_N \;=\; \frac{N}{T}. \tag{6}$$

Note that by construction C is of rank $\min\{N, T\}$, therefore it will have exactly $N - T$ zero eigenvalues if $T < N$. In the following we consider a large N limit, such that N/T is finite, so that the matrix C will never be deterministic. Since by definition ξ is a positive definite matrix, therefore η can not be chosen arbitrarily.

We are interested in the statistics of the eigenvalues of C. For instance, the eigenvalue density, $\rho_{\mathsf{C}}(z, z^*)$, which is defined as

$$\rho_{\mathsf{C}}(z, z^*) = \frac{1}{N}\sum_{j=1}^{N} \delta(z - \lambda_j)\delta(z^* - \lambda_j^*), \tag{7}$$

where z^* stands for the complex conjugate of z. We use *overbar* to represent the ensemble averaged density and also for other ensemble averaged quantities. The density can be obtained from the Green's function, $\overline{\mathsf{g}}_{\mathsf{C}}(z, z^*)$, via

$$\overline{\rho}_{\mathsf{C}}(z, z^*) = \frac{1}{\pi}\frac{\partial \overline{\mathsf{g}}_{\mathsf{C}}(z, z^*)}{\partial z^*}, \tag{8}$$

where

$$\overline{\mathsf{g}}_{\mathsf{C}}(z, z^*) = \lim_{\epsilon \to 0} \left\langle \overline{\frac{z^*\mathbf{1}_N - \mathsf{C}^t}{(z^*\mathbf{1}_N - \mathsf{C}^t)(z\mathbf{1}_N - \mathsf{C}) + \epsilon^2 \mathbf{1}_N}} \right\rangle. \tag{9}$$

In the above definition we have introduced the spectral averaging, using the angular brackets as $\langle \mathsf{H} \rangle = \mathrm{tr}\,\mathsf{H}/K$, for a $K \times K$ matrix H.

Often the above definitions are described better as an analogy of two-dimensional electrostatics [41–43]. For instance, the *potential* in this case is $F(z, z^*) = \ln(\mathrm{Det}(z^* - \mathsf{C}^t)(z - \mathsf{C}) + \epsilon^2)$. The thus analogous *electric field* will then be $\overline{\mathsf{g}}_{\mathsf{C}}(z, z^*)$. Finally, $\overline{\rho}_{\mathsf{C}}(z, z^*)$ will be the charge density as a consequence of the two-dimensional Gauss law (8).

In order to evaluate $\overline{\mathsf{g}}_{\mathsf{C}}(z, z^*)$ for large N, one is tempted to use the methods developed for the Hermitian matrices, e.g., planer diagram method [20, 43, 46] or the binary correlation method [13, 24, 33, 47]. However, the large z-expansion consist of nonlinear combinations of C and C^t and these combinations make direct applications of such methods very complicated. As in [45], to circumvent this problem we rather calculate a $2N \times 2N$ matrix, $\overline{\mathbf{G}}(z, z^*)$, defined as

$$\overline{\mathbf{G}}(z, z^*) = \lim_{\epsilon \to 0} \overline{\begin{pmatrix} z\mathbf{1}_N - \mathsf{C} & \mathrm{i}\epsilon\mathbf{1}_N \\ \mathrm{i}\epsilon\mathbf{1}_N & z^*\mathbf{1}_N - \mathsf{C}^t \end{pmatrix}^{-1}}. \tag{10}$$

Note that $\overline{\mathsf{g}}_{\mathsf{C}}(z, z^*)$ will be the spectral-averaged first diagonal block of a $\overline{\mathbf{G}}(z, z^*)$. Now our goal is to calculate $\overline{\mathbf{G}}(z, z^*)$ which is still complicated. To simplify the problem, we use a trick of linearization as proposed in Ref. [42], so all the non-vanishing contributions be appropriately taken into account extending the binary correlation

method used for the Gaussian ensembles [47]. We emphasize that our results are valid in the same limit as has been addressed in Ref. [34].

III. THE LOOP EQUATION

We begin with linearizing the problem, defining an $(N+T)\times(N+T)$ dimensional matrix P as

$$\mathsf{P} = \frac{1}{\sqrt{T}}\begin{pmatrix}\mathbf{0} & \mathsf{A}\\ \mathsf{B}^t & \mathbf{0}\end{pmatrix}. \tag{11}$$

With a note that the nonzero eigenvalues of P^2 coincide with the nonzero eigenvalues of C [45] and have a two-fold degeneracy for each, so we calculate $\overline{\rho}_{\mathsf{C}}(z,z^*)$ from the spectral density, $\overline{\rho}_{\mathsf{P}}(w,w^*)$, of P, using

$$\overline{\rho}_{\mathsf{C}}(z,z^*) = \frac{1}{2|z|}\overline{\rho}_{\mathsf{P}}(w(z),w^*(z^*)). \tag{12}$$

Here $z=w^2$. Another very useful relation is between the corresponding Green's functions:

$$z\overline{\mathsf{g}}_{\mathsf{C}}(z,z^*) - 1 = \frac{T+N}{2N}\left[w\overline{\mathsf{g}}_{\mathsf{P}}(w(z),w^*(z^*)) - 1\right], \tag{13}$$

where $\overline{\mathsf{g}}_{\mathsf{P}}(w,w^*)$ is the Green's function of $\overline{\rho}_{\mathsf{P}}(w(z),w^*(z^*))$. As it will be shown later, we first derive $\overline{\mathsf{g}}_{\mathsf{P}}(w,w^*)$ and consequently $\overline{\mathsf{g}}_{\mathsf{C}}(z,z^*)$ using the above relations.

Following the definition (10), we define a $2(N+T)\times 2(N+T)$ dimensional matrix $\tilde{\mathsf{P}}$ as

$$\tilde{\mathsf{P}} = \begin{pmatrix}\mathsf{P} & \mathbf{0}\\ \mathbf{0} & \mathsf{P}^t\end{pmatrix}. \tag{14}$$

The corresponding Green's function $\tilde{\mathsf{G}}$ can then be written as

$$\tilde{\mathsf{G}}(w,w^*) = \left(\tilde{\mathsf{W}} - \tilde{\mathsf{P}}\right)^{-1}, \tag{15}$$

where

$$\tilde{\mathsf{W}} = \begin{pmatrix}w\,\mathbf{1}_{N+T} & \mathrm{i}\epsilon\mathbf{1}_{N+T}\\ \mathrm{i}\epsilon\mathbf{1}_{N+T} & w^*\,\mathbf{1}_{N+T}\end{pmatrix}. \tag{16}$$

It is suggestive to write $\tilde{\mathsf{G}}$ in terms of smaller blocks

$$\overline{\tilde{\mathsf{G}}} = \begin{pmatrix}\overline{\mathsf{G}}_{11} & \overline{\mathsf{G}}_{12} & \overline{\mathsf{G}}_{1\overline{1}} & \overline{\mathsf{G}}_{1\overline{2}}\\ \overline{\mathsf{G}}_{21} & \overline{\mathsf{G}}_{22} & \overline{\mathsf{G}}_{2\overline{1}} & \overline{\mathsf{G}}_{2\overline{2}}\\ \overline{\mathsf{G}}_{\overline{1}1} & \overline{\mathsf{G}}_{\overline{1}2} & \overline{\mathsf{G}}_{\overline{1}\overline{1}} & \overline{\mathsf{G}}_{\overline{1}\overline{2}}\\ \overline{\mathsf{G}}_{\overline{2}1} & \overline{\mathsf{G}}_{\overline{2}2} & \overline{\mathsf{G}}_{\overline{2}\overline{1}} & \overline{\mathsf{G}}_{\overline{2}\overline{2}}\end{pmatrix}, \tag{17}$$

where $\overline{\mathsf{G}}_{jj}$ and $\overline{\mathsf{G}}_{\overline{j}\overline{j}}$ are $N\times N$ and $T\times T$ respectively for the block indices $j=1$ and 2, and the overbar are used again, but for integers, to represent the blocks.

In order to perform the ensemble averaging we expand $\overline{\tilde{\mathsf{G}}}$ for large w:

$$\overline{\tilde{\mathsf{G}}} = \tilde{\mathsf{W}}^{-1} + \tilde{\mathsf{W}}^{-1}\overline{\tilde{\mathsf{P}}\tilde{\mathsf{W}}^{-1}\tilde{\mathsf{P}}\tilde{\mathsf{W}}^{-1}} + \dots\ . \tag{18}$$

As in the case of symmetric correlation matrices [24], we collect only the leading order terms and avoid those resulting in $\mathcal{O}(N^{-1})$ or smaller. Using the jpd (1), we first derive the following exact identities, valid for arbitrary fixed matrices χ_1 and χ_2:

$$\frac{1}{T}\overline{\mathsf{A}\chi_1\mathsf{A}^t\chi_2} = \langle\chi_1\rangle\,\chi_2, \tag{19}$$

$$\overline{\mathsf{A}\chi_1\mathsf{A}\chi_2} = \chi_2\chi_1^t, \tag{20}$$

$$\frac{1}{T}\overline{\mathsf{B}\chi_1\mathsf{B}^t\chi_2} = \langle\chi_1\rangle\,\chi_2, \tag{21}$$

$$\overline{\mathsf{B}\chi_1\mathsf{B}\chi_2} = \chi_2\chi_1^t. \tag{22}$$

These identities are sufficient to obtain results for the $\eta=0$ case. However, for $\eta\neq 0$, we further derive

$$\frac{1}{T}\overline{\mathsf{A}\chi_1\mathsf{B}^t\chi_2} = \langle\chi_1\rangle\,\eta\chi_2, \tag{23}$$

$$\frac{1}{T}\overline{\mathsf{A}^t\chi_1\mathsf{B}\chi_2} = \kappa\,\langle\eta^t\chi_1\rangle\,\chi_2, \tag{24}$$

$$\frac{1}{T}\overline{\mathsf{B}\chi_1\mathsf{A}^t\chi_2} = \langle\chi_1\rangle\,\eta^t\chi_2, \tag{25}$$

$$\frac{1}{T}\overline{\mathsf{B}^t\chi_1\mathsf{A}\chi_2} = \kappa\,\langle\eta\chi_1\rangle\,\chi_2. \tag{26}$$

In what follows, we ignore lower order terms in the ensemble averaging while keeping only the leading order terms. Using the identities (19, 21) and (23-26), i.e., avoiding terms resulting from the binary associations of A with A or with B or of B with B or with A, we obtain

$$\overline{\tilde{\mathsf{G}}} = \left(\tilde{\mathsf{W}} - \Sigma\right)^{-1}, \tag{27}$$

where

$$\Sigma = \begin{pmatrix}\langle\overline{\mathsf{G}}_{22}\rangle\eta & \mathbf{0} & \langle\overline{\mathsf{G}}_{2\overline{2}}\rangle\mathbf{1}_N & \mathbf{0}\\ \mathbf{0} & \kappa\langle\eta\overline{\mathsf{G}}_{11}\rangle\mathbf{1}_T & \mathbf{0} & \kappa\langle\overline{\mathsf{G}}_{1\overline{1}}\rangle\mathbf{1}_T\\ \langle\overline{\mathsf{G}}_{\overline{2}2}\rangle\mathbf{1}_N & \mathbf{0} & \langle\overline{\mathsf{G}}_{\overline{2}\overline{2}}\rangle\eta^t & \mathbf{0}\\ \mathbf{0} & \kappa\langle\overline{\mathsf{G}}_{\overline{1}1}\rangle\mathbf{1}_T & \mathbf{0} & \kappa\langle\overline{\eta^t\mathsf{G}}_{\overline{1}\overline{1}}\rangle\mathbf{1}_T\end{pmatrix}. \tag{28}$$

Notice that avoiding the lower order contributions yields zeros in the rectangular blocks. Finally, calculating the inverse in Eq. (27), we obtain

$$\overline{\tilde{\mathsf{G}}} = \begin{pmatrix}\overline{\Gamma}_1^{(1)}\mathsf{d}_1 & \mathbf{0} & \overline{\Gamma}_1^{(1)}\langle\overline{G}_{2\overline{2}}\rangle & \mathbf{0}\\ \mathbf{0} & \overline{\Gamma}_1^{(2)}\mathsf{d}_2 & \mathbf{0} & \kappa\overline{\Gamma}_1^{(2)}\langle\overline{G}_{1\overline{1}}\rangle\\ \overline{\Gamma}_2^{(1)}\langle\overline{G}_{\overline{2}2}\rangle & \mathbf{0} & \overline{\Gamma}_2^{(1)}\mathsf{a}_1 & \mathbf{0}\\ \mathbf{0} & \kappa\overline{\Gamma}_2^{(2)}\langle\overline{G}_{\overline{1}1}\rangle & \mathbf{0} & \overline{\Gamma}_2^{(2)}\mathsf{a}_2\end{pmatrix}. \tag{29}$$

Here,

$$\overline{\Gamma}_1^{(1)} = \left[\overline{\mathsf{d}}_1\overline{\mathsf{a}}_1 - \overline{g}_{2\overline{2}}\overline{g}_{\overline{2}2}\mathbf{1}_N\right]^{-1}, \tag{30}$$

$$\overline{\Gamma}_2^{(1)} = \left[\overline{\mathsf{a}}_1\overline{\mathsf{d}}_1 - \overline{g}_{2\overline{2}}\overline{g}_{\overline{2}2}\mathbf{1}_N\right]^{-1}, \tag{31}$$

$$\overline{\Gamma}_1^{(2)} = \left[\overline{\mathsf{d}}_2\overline{\mathsf{a}}_2 - \kappa^2\overline{g}_{1\overline{1}}\overline{g}_{\overline{1}1}\mathbf{1}_T\right]^{-1}, \tag{32}$$

$$\overline{\Gamma}_2^{(2)} = \left[\overline{\mathsf{a}}_2\overline{\mathsf{d}}_2 - \kappa^2\overline{g}_{1\overline{1}}\overline{g}_{\overline{1}1}\mathbf{1}_T\right]^{-1}, \tag{33}$$

and

$$\overline{\mathsf{a}}_1 = w\mathbf{1}_N - \overline{g}_{22}\eta,\ \overline{\mathsf{d}}_1 = w^*\mathbf{1}_N - \overline{g}_{\overline{2}\overline{2}}\eta^t, \tag{34}$$

$$\overline{\mathsf{a}}_2 = (w - \kappa\overline{g}_{11,\eta})\mathbf{1}_T,\ \overline{\mathsf{d}}_2 = (w^* - \kappa\overline{g}_{\overline{1}\,\overline{1},\eta^t})\mathbf{1}_T. \tag{35}$$

Some details of the derivation of the above equation are given in Appendix A.

In the above result we have used rather more general spectral-averaging, viz.,

$$\overline{g}_{jj,\mathsf{L}} = \langle \mathsf{L}\overline{\mathsf{G}}_{jj}\rangle,\ \overline{g}_{\overline{j}\,\overline{j},\mathsf{L}} = \langle \mathsf{L}\overline{\mathsf{G}}_{\overline{j}\,\overline{j}}\rangle, \tag{36}$$

where L is $N\times N$ and $T\times T$, respectively for $j=1$ and 2. For instance, in Eq. (35), we have considered $\mathsf{L}=\eta$ and η^t, respectively in the first and the second equality. Next, on equating the right hand sides of Eqs. (17) and (29), we derive a set of coupled equations. For instance, on comparing spectral averages of the diagonal blocks we obtain

$$\overline{g}_{11} = \langle \overline{\Gamma}_1^{(1)}\overline{\mathsf{d}}_1\rangle,\ \overline{g}_{22} = \langle \overline{\Gamma}_1^{(2)}\overline{\mathsf{d}}_2\rangle, \tag{37}$$

$$\overline{g}_{\overline{1}\,\overline{1}} = \langle \overline{\Gamma}_2^{(1)}\overline{\mathsf{a}}_1\rangle,\ \overline{g}_{\overline{2}\,\overline{2}} = \langle \overline{\Gamma}_2^{(2)}\overline{\mathsf{a}}_2\rangle. \tag{38}$$

Similarly, averaging over the off-diagonal blocks gives

$$\overline{g}_{1\overline{1}} = \overline{g}_{2\overline{2}}\langle \overline{\Gamma}_1^{(1)}\rangle,\ \overline{g}_{\overline{1}1} = \overline{g}_{\overline{2}2}\langle \overline{\Gamma}_2^{(1)}\rangle, \tag{39}$$

$$\overline{g}_{2\overline{2}} = \kappa\overline{g}_{1\overline{1}}\langle \overline{\Gamma}_1^{(2)}\rangle,\ \overline{g}_{\overline{2}2} = \kappa\overline{g}_{\overline{1}1}\langle \overline{\Gamma}_2^{(2)}\rangle. \tag{40}$$

All together the Eqs. (37,38,39,40) are the loop equations for P. Eliminating $\overline{g}_{1\overline{1}}$ and $\overline{g}_{\overline{1}1}$ from Eqs. (39,40) we get an important identity:

$$\langle \overline{\Gamma}_j^{(1)}\rangle\,\langle \overline{\Gamma}_j^{(2)}\rangle = \frac{1}{\kappa}, \tag{41}$$

for $j=1,2$. The Green's function, which describes the spectral density for P, is given by

$$\overline{\mathsf{g}}_{\mathsf{P}}(w,w^*) = \frac{N\,\overline{g}_{11}(w,w^*) + T\,\overline{g}_{22}(w,w^*)}{N+T}. \tag{42}$$

As in the previous cases [34, 42], here we obtain two solutions for $\overline{g}_{jj}$. For the trivial one, $\overline{g}_{\overline{j}j}$ and $\overline{g}_{j\overline{j}}$ are 0. This solution corresponds to the holomorphic region as for large w the Green's function behaves as $1/w$. The other solution is a nontrivial, giving $\overline{\mathsf{g}}_{\mathsf{P}}(w,w^*)$, and consequently $\overline{\mathsf{g}}_{\mathsf{C}}(z,z^*)$ for which the Gauss law (8) gives the density we desire in the nonholomorphic region. For infinitely large matrices, however, the density has a sharp cut-off at the boundary of holomorphic and the nonholomorphic regions.

IV. THE DOMAIN OF EIGENVALUES

For a general η, an analytic solution in the nonholomorphic region is difficult to obtain. However, the situation is simpler at the boundary of the holomorphic-nonholomorphic region. As in Refs. [34, 42, 44, 45], we match the solution of nonholomorphic and holomorphic regions and derive a formula for the contours defining such boundaries. On the boundary, we use $\overline{g}_{j\overline{j}} = \overline{g}_{\overline{j}j} = 0$ in Eqs. (30-33) and obtain

$$\langle \overline{\Gamma}_1^{(1)}\rangle = \langle \big[\overline{\mathsf{d}}_1\overline{\mathsf{a}}_1\big]^{-1}\rangle = \langle \overline{\Gamma}_2^{(1)}\rangle \equiv \overline{\gamma}_1, \tag{43}$$

$$\langle \overline{\Gamma}_1^{(2)}\rangle = \langle \big[\overline{\mathsf{d}}_2\overline{\mathsf{a}}_2\big]^{-1}\rangle = \langle \overline{\Gamma}_2^{(2)}\rangle \equiv \overline{\gamma}_2. \tag{44}$$

Next, we simplify Eqs. (37, 38) using $\overline{g}_{j\overline{j}} = \overline{g}_{\overline{j}j} = 0$ and the definition (36), for $\overline{g}_{11,\eta}$. This method leads to a self-consistent equation:

$$\overline{g}_{11,\eta} = (w - \kappa\overline{g}_{11,\eta})\left\langle \eta\left(w(w-\kappa\overline{g}_{11,\eta}) - \eta\right)^{-1}\right\rangle. \tag{45}$$

Denoting $w(w-\kappa\overline{g}_{11,\eta}) = \Psi$ one can cast this equation into

$$z = \Psi + \kappa\Psi\left\langle \eta\left(\Psi - \eta\right)^{-1}\right\rangle, \tag{46}$$

where we have replaced w^2 by z. Similarly, for $\overline{g}_{\overline{1}\,\overline{1},\eta^t}$, we obtain

$$z^* = \Psi^* + \kappa\Psi^*\left\langle \eta^t\left(\Psi^* - \eta^t\right)^{-1}\right\rangle. \tag{47}$$

Next, from the identity (41) we obtain an equation for Ψ:

$$\langle[(\Psi-\eta)(\Psi^*-\eta^t)]^{-1}\rangle = \frac{1}{\kappa}. \tag{48}$$

Equation (46), describes the contour enclosing bulk of the eigenvalues in terms of the solution Ψ of the Eq. (48). Let η be commuting with η^t. Then Eq. (48) has eigenvalue expansion and thus can be simplified in terms of the eigenvalues of η; see Sec. V. On the other hand if η does not commute with η^t then the Eq. (48) does not have further simplifications. The underlying remark for the latter case is that solution of Eq. (48) depends on η_S and η_A, where $\eta_S = (\eta+\eta^t)/2$ and $\eta_A = (\eta-\eta^t)/2$ are the symmetric and anti-symmetric parts of η. Therefore the contour (46) as well depends on the symmetric and the anti-symmetric parts of η.

V. EXAMPLES

In examples, we consider η to be a tridiagonal matrix. We consider $\eta_{jk} = c\,\delta_{jk} + p\,\delta_{j,k+1} + q\,\delta_{j+1,k}$, where $\ell = N+1 \equiv 1$ is defined via cyclic convention and c, p, q are real. The eigenvalues, $\lambda_j^{(\eta)}$, of η, are given by [48]

$$\lambda_j^{(\eta)} = c + 2\sqrt{pq}\cos(\frac{j\pi}{N+1}), \tag{49}$$

for $1\le j\le N$. We choose c and p,q such that $\lambda_j^{(\eta)} < 1$, so that the positive definiteness of ξ is ensured. Let $p=q$.

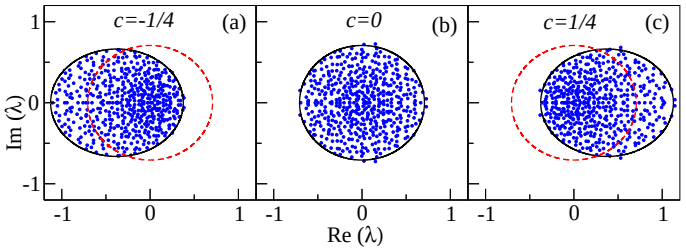

FIG. 1: (Color online) Scatter plot for the eigenvalues for the case (i), where η is diagonal with the same entries c. Here data, (eigenvalues) obtained from the diagonalization of the corresponding matrix C, are represented by dots and theory (55) is represented by the solid lines. In this figure the matrix dimension $N = 512$ where we show only 1 realization.

Then using $\lambda_j^{(\eta)}$ in Eq. (46), we write

$$z = \Psi(1-\kappa) + \kappa\Psi^2 \sum_{j=1}^{N} \frac{1}{N\left(\Psi - c - 2c_0\cos\left(\frac{j\pi}{N+1}\right)\right)}, \tag{50}$$

where $c_0 = |\sqrt{pq}|$. For large N, the summation may be replaced by an integral. Solving this integral by using the technique of contour integration, we obtain

$$z = \Psi(1-\kappa) + \frac{\kappa\Psi^2}{\sqrt{(\Psi-c)^2 - 4c_0^2}}. \tag{51}$$

Similarly, from (48) we get

$$\frac{1}{k} + \frac{2rs\cos(\theta-\nu)}{8c_0^2r^2\cos(2\theta) - [16c_0^4 + r^4 - s^2(4c_0^2 - r^2)]} = 0, \tag{52}$$

where

$$\Psi - c = r\exp(\mathrm{i}\theta), \text{ and } \sqrt{r^2\exp(2\mathrm{i}\theta) - 4c_0^2} = s\exp(\mathrm{i}\nu). \tag{53}$$

We consider five cases for this tridiagonal matrix, viz., (i) $c \neq 0$ and $p = q = 0$, (ii) $p = q \neq 0$, (iii) $c = 0$, $p = -q$, (iv) $c \neq 0$, $p = -q$, and (v) $c \neq 0$, $p \neq q$. Note that for the cases (i, ii) η is symmetric and for the case (iii) it is anti-symmetric. In the case (iv) η is nonsymmetric but commutes with η^t while in (v) η is nonsymmetric and does not commute with η^t. In the final example, our result (48) can not be simplified to the eigenvalues and consequently Eq. (52) does not apply. However, for the remaining cases the latter can be used.

For the case (i) Eq. (52) yields a circle, i.e., $|\Psi - c|^2 = \kappa$. Using the solution of (51) for this circle, we get

$$\left|z - c(1+\kappa) + \sqrt{[z-c(1+\kappa)]^2 - 4c^2\kappa}\right|^2 = 4\kappa. \tag{54}$$

Let $z = x + \mathrm{i}y$. Then an ellipse can be observed from the above equation by shifting the x-axis, defining $Z = X + \mathrm{i}Y$, where $X = x - c(1+\kappa)$ and $Y = y$, and then rescaling X and Y as $\phi = u + \mathrm{i}v$ where $u = X/\sqrt{\kappa}(1+c^2)$ and $v = Y/\sqrt{\kappa}(1-c^2)$. Since Eq. (54) is satisfied for $|\phi| = 1$, the solution for z satisfying equation (54) is an ellipse:

$$\frac{(x - c(1+\kappa))^2}{\kappa(1+c^2)^2} + \frac{y^2}{\kappa(1-c^2)^2} = 1. \tag{55}$$

In Sec. VI we explicitly calculate spectral density for this case.

In Fig. 1 we compare this results for different c with eigenvalues obtained from diagonalizing $N = 512$ dimensional matrix. In this figure we show results for $c = -1/4, 0$ and $1/4$ respectively in (a), (b) and (c). For $c = 0$ the eigenvalues are enclosed by a circle of radius $\sqrt{\kappa}$ while for $c = -1/4$ and for $c = 1/4$ these are enclosed by shifted ellipses calculated from (55).

We observe that for given c_0, (52) is the same for the cases (ii), (iii) and (iv), and only (51) may differ. For instance, in the case (ii) Eq. (51) remains the same but for the remaining two cases we have

$$z = \Psi'(1-\kappa) + \frac{\kappa\Psi'^2}{\mathrm{i}\sqrt{\Psi^2 - 4c_0^2}}, \tag{56}$$

where $\Psi' = \mathrm{i}\Psi + c$. For example, in the case (iii) we have $\Psi' = \mathrm{i}\Psi$ which gives the same contour representing its symmetric counterpart but with a change in phase by $\pi/2$. In Fig. 2, we compare our theory with numerics for $N = 512$ where $c = 1/4$ and c_0 is varied from $c_0 = 1/4$ to $3/8$. As shown in the figure, the contours are symmetric along the y-axis but not along the x-axis. This asymmetry arises from the nonzero choice of c. For

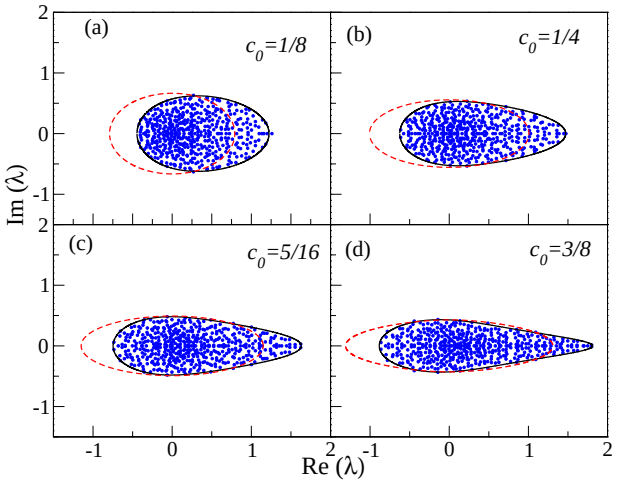

FIG. 2: (Color online) Scatter plot for the eigenvalues of C corresponding symmetric η described as the case (ii) in the text. Data (eigenvalues) obtained from the diagonalization of C are represented by dots and theories (51) are represented by solid lines. We have compared theory with numerics for $c = 1/4$ and $c_0 = 1/8$, $1/4$, $5/16$ and $3/8$ respectively in (a), (b), (c) and (d). Dashed *red* lines represent contours for $c = 0$ the corresponding c_0 values. In this figure the matrix dimension $N = 512$ where we show only 1 realization.

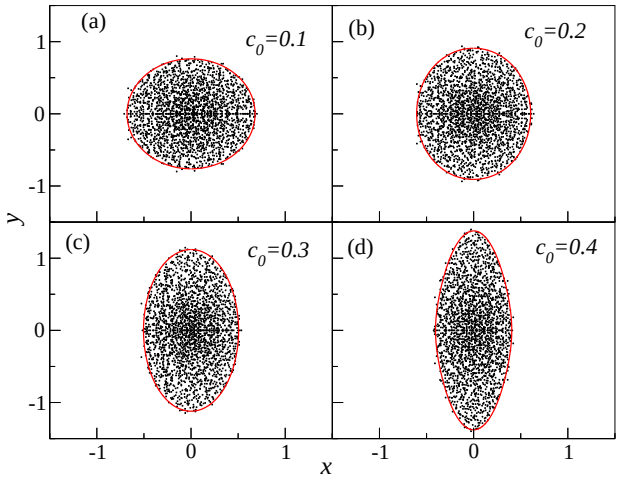

FIG. 3: (Color online) Scatter plot for the eigenvalues of C corresponding anti-symmetric η described as the case (iii) in the text. Data (eigenvalues) obtained from the diagonalization of C are represented by dots and theory (56) is represented by the solid lines. In this figure the matrix dimension $N = 384$ where we show 6 independent realizations.

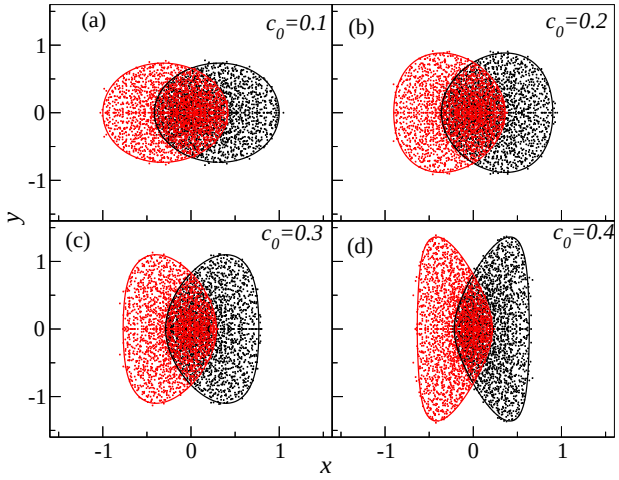

FIG. 4: (Color online) Scatter plot for the eigenvalues of C corresponding nonsymmetric but commuting η described as the case (iv) in the text. Data (eigenvalues) obtained from the diagonalization of C are represented by dots and theory (56) is represented by the solid lines. Black lines represent contours for $c = 0.2$ and red lines represent contours for $c = -0.2$. For both values we have considered $c_0 = 0.1\,0.2\,0.3$ and 0.4 respectively in (a,b,c) and (d). In this figure the matrix dimension $N = 384$ where we show data for 6 independent realizations.

comparison, we also show the result for $c = 0$ where the contour has symmetry along the x-axis.

In Fig. 3, we vary c_0 from 0.1 to 0.4 to compare our theory with numerics for the case (iii). As it is evident from the theory, in this case the contours are symmetric along the both axis. For the nonsymmetric but commuting η and η^t, i.e., the case (iv), we show the results in Fig. 4 where c_0 is varied in the same range. Here we

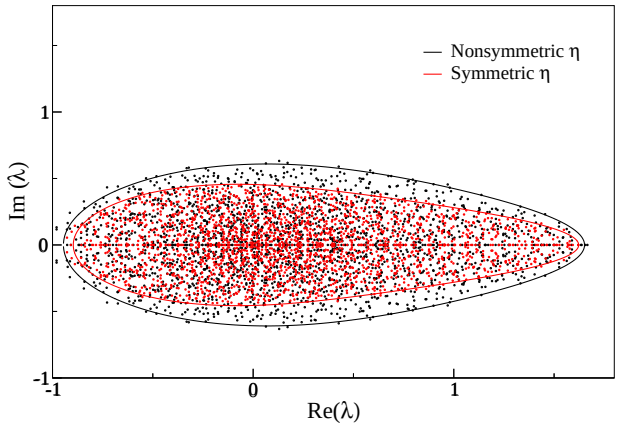

FIG. 5: (Color online) Scatter plot for the eigenvalues of C corresponding non-commuting η, described as the case (v) in the text. Data (eigenvalues) obtained from the diagonalization of C are represented by dots and theory (46) is represented by the solid lines. Black lines represent contours for the nonsymmetric η and red lines represent contours for the symmetric η with the same spectrum. Result for nonsymmetric case is shown for $c = 0.2$, $p = 0.2$ and $q = 0.6$, and for the symmetric case these are shown for $c = 0.2$, $p = q = \sqrt{0.12}$. In this figure the matrix dimension $N = 384$ and we show 6 independent realizations.

have considered $c = 0.2$ and -0.2, shown respectively by black and red colors. As shown in the figure, our theory gives reasonable account of the eigenvalue domain.

Finally, for the case (v), we consider $c = 0.2$, $p = 0.2$ and $q = 0.6$ and $N = 384$. Since in this case η does not commute with η^t, Eq. (48) has to be solved numerically. In Fig. 5, we compare this solution with the data obtained from the matrix diagonalization. For the numerical solution of Eq. (48), we consider $N = 512$. As shown in the figure, our theory closely predicts the boundary. For comparison we also plot the contour which describes the boundary for the symmetric η which has the same spectrum. This figure confirms that the boundaries are sensitive to the nonsymmetry in the correlation matrix η as opposed to the symmetric or anti-symmetric cases where it depends only on the spectrum of η. Also the singular values are sensitive to the nonsymmetry. In Fig. 6 we compare densities of the square of the singular values of C for the same symmetric and nonsymmetric η. This figure confirms that the nonsymmetry can also be observed in the singular values of C but in the tail.

VI. THE DENSITY OF EIGENVALUES: SOME ESPECIAL CASES

Let $\eta = 0$. Then from Eqs. (34-35), we have $\mathsf{a}_1 = w\mathbf{1}_N$, $\mathsf{a}_2 = w\mathbf{1}_T$, $\mathsf{d}_1 = w^*\mathbf{1}_N$ and $\mathsf{d}_2 = w^*\mathbf{1}_T$. These will lead to the same set of equations as obtained in Ref. [34] for the uncorrelated matrices. On the other hand, for $\eta \neq 0$, these equations are very complicated. Analytically,

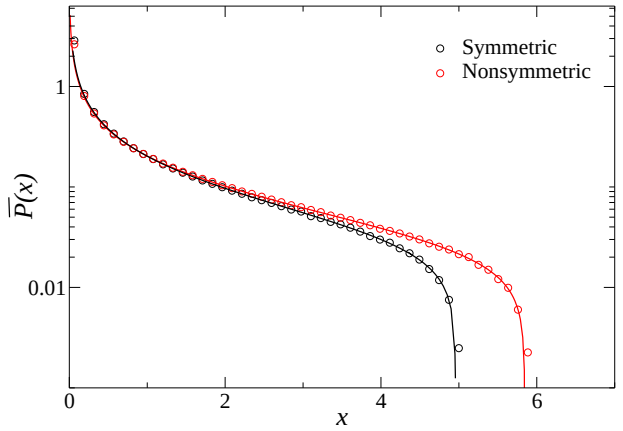

FIG. 6: (Color online) Density, $\overline{P}(x)$, vs x where x is the square of the singular values of C corresponding η of the case (v). In this figure we use the same η as has been used in Fig. 5. In this case the density depends on the spectrum of $\eta\eta^t$ instead of η [33]. Data obtained from the singular value decomposition of C are shown by open circles and theories are shown by solid lines. Black lines and circles stand for the symmetric η while red ones represent results for the non-symmetric η. We have used 100 spectrum of 512 dimensional matrices to obtain this density.

however, these can be solved if there is a relation between $\langle\overline{\Gamma}_j^{(1)}\rangle$ and $\langle\overline{\Gamma}_j^{(2)}\rangle$. In the examples we consider below we exploit this fact and derive the spectral densities for some especial cases of η.

In the first case we consider $\eta_{jk} = c$ where $0 \leq c \leq 1/N$. This choice defines the equal-cross-correlation matrix model. In this case η is rank one, therefore it has only one nonzero eigenvalue Nc. On the other hand for the bulk of the spectrum [49], we have $\mathsf{a}_1 = w\mathbf{1}_N$, $\mathsf{a}_2 = w\mathbf{1}_T$, $\mathsf{d}_1 = w^*\mathbf{1}_N$ and $\mathsf{d}_2 = w^*\mathbf{1}_T$. These will lead to the same set of equations as for the uncorrelated case. Therefore, for the bulk we know the result. For instance, using the result (55) we know that the contour enclosing the bulk is defined by a circle of radius $\sqrt{\kappa}$. However, the spectrum may have one eigenvalue lying off the circle. The ensemble averaged position of this eigenvalue is $\sim Nc$ provided $Nc > \sqrt{\kappa}$. Such observations have been very useful in the analysis of symmetric correlation matrices [4–7] and also of the density matrices [50]. On the other hand, we also have an upper bound $Nc < 1$ due to the positive definiteness of ξ which consequently implies that there will be no eigenvalue separation from the bulk for $\kappa > 1$.

For the second case we consider $\eta_{jk} = c\,\delta_{jk}$. Using Eqs. (34-35) and Eqs. (36-40), we get

$$\begin{aligned}\overline{\mathsf{a}}_1 &= (w - c\,\overline{g}_{22})\mathbf{1}_N,\ \overline{\mathsf{a}}_2 = (w - \kappa\, c\,\overline{g}_{11})\mathbf{1}_T \\ \overline{\mathsf{d}}_1 &= (w^* - c\,\overline{g}_{\overline{2}\,\overline{2}})\mathbf{1}_N,\ \overline{\mathsf{d}}_2 = (w^* - \kappa\, c\,\overline{g}_{\overline{1}\,\overline{1}})\mathbf{1}_T. \quad (57)\end{aligned}$$

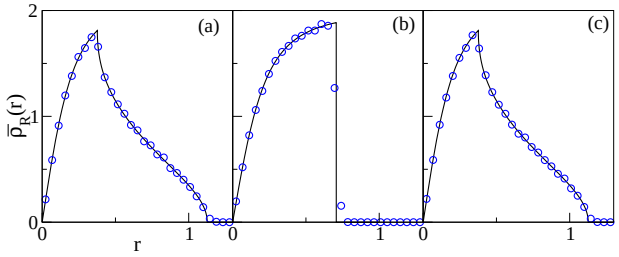

FIG. 7: (Color online) Radial distribution, $\overline{\rho}_{\mathsf{R}}(r)$, of the densities of absolute values of the spectra of C corresponding the $\eta_{jk} = c\delta_{jk}$ case. In this figure we show results for $c = -1/4$, 0 and $1/4$ respectively in (a), (b) and (c). The corresponding scatter plots of these are shown respectively in Fig. 1(a), (b) and (c). Theory for $\overline{\rho}_{\mathsf{R}}(r)$ is obtained by integrating the θ-variable of (69) in the domain described by (55), where $z = r\,\exp(\mathrm{i}\theta)$. In this figure the matrix dimension $N = 512$ where we have used 300 independent realizations to obtain the result.

Next, from Eqs. (30-33) we get

$$\langle\overline{\Gamma}_1^{(1)}\rangle = \langle\overline{\Gamma}_2^{(1)}\rangle = \left\langle \frac{1}{\overline{\mathsf{a}}_1\,\overline{\mathsf{d}}_1 - \overline{g}_{2\overline{2}}\overline{g}_{\overline{2}2}\mathbf{1}_N} \right\rangle \equiv \overline{\gamma}_1, \quad (58)$$

$$\langle\overline{\Gamma}_1^{(2)}\rangle = \langle\overline{\Gamma}_2^{(2)}\rangle = \left\langle \frac{1}{\overline{\mathsf{a}}_2\,\overline{\mathsf{d}}_2 - \kappa^2\overline{g}_{1\overline{1}}\overline{g}_{\overline{1}1}\mathbf{1}_T} \right\rangle \equiv \overline{\gamma}_2. \quad (59)$$

Using these in Eqs. (37-40), the set of equations we obtain is

$$\overline{g}_{jj} = \overline{\mathsf{d}}_j\overline{\gamma}_j,\ \overline{g}_{\overline{j}\,\overline{j}} = \overline{\mathsf{a}}_j\overline{\gamma}_j, \quad (60)$$

and

$$\begin{aligned}\overline{g}_{1\overline{1}} = \overline{g}_{2\overline{2}}\overline{\gamma}_1,\ \overline{g}_{2\overline{2}} = \kappa\overline{g}_{1\overline{1}}\overline{\gamma}_2, \\ \overline{g}_{\overline{1}1} = \overline{g}_{\overline{2}2}\overline{\gamma}_1,\ \overline{g}_{\overline{2}2} = \kappa\overline{g}_{\overline{1}1}\overline{\gamma}_2. \quad (61)\end{aligned}$$

Finally, the identity (41) gives

$$\overline{\gamma}_1\overline{\gamma}_2 = \frac{1}{\kappa}. \quad (62)$$

In the holomorphic region, these equations have a simple solution, viz., $\overline{g}_{j\overline{j}} = \overline{g}_{\overline{j}j} = 0$. In the nonholomorphic region, which is described by the ellipse (55), we solve this equations by observing a linear relation between the $\overline{\gamma}_j$'s. However, to be consistent with the notation used in Ref. [34], we instead use $\overline{\mu}_j$ for $|w|^2\overline{\gamma}_j - 1$, for $j = 1, 2$. Using the identity (62) and after some algebra, in this case we indeed obtain a linear relation between the $\overline{\mu}_j$s:

$$\overline{\mu}_2 = -c^2(1-\kappa) + \kappa\overline{\mu_1}. \quad (63)$$

Note that together with the identity (62), the above relation simplifies the problem to a quadratic equation since the Green's function, we wish to calculate in side the ellipse (55), is given by

$$\overline{\mathsf{g}}_{\mathsf{C}}(z, z^*) = \frac{\kappa\overline{\mu}_1 + \overline{\mu}_2 + (\kappa+1)\,c^2 - 2cz + 2(1-c^2)\kappa}{2(1-c^2)\kappa z}. \quad (64)$$

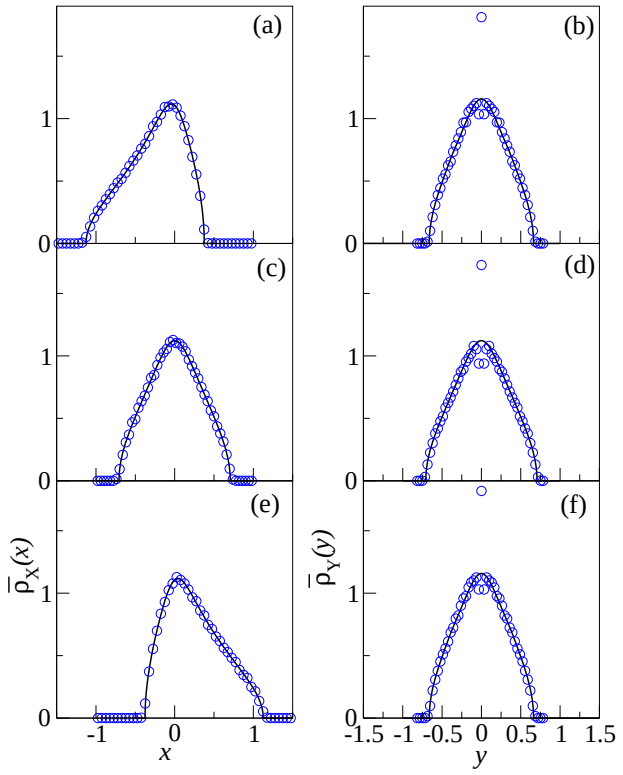

FIG. 8: (Color online) Marginal distributions $\overline{\rho}_X(x)$ and $\overline{\rho}_Y(y)$ describing respectively the densities of real and imaginary part of the eigenvalues for the $\eta_{jk} = c\delta_{jk}$ case. In this figure we consider $c = -1/4$, 0 and $1/4$ from top to bottom. The corresponding scatter plots of these are shown respectively in Fig. 1(a), (b) and (c). Theory for $\overline{\rho}_X(x)$ is obtained from the integration of the y-variable in (69) in the domain described by an ellipse (55). Similarly $\overline{\rho}_Y(y)$ is obtained by integrating over the x-variable in the same domain. In this figure the matrix dimension $N = 512$ where we have used 300 independent realizations to obtain the result.

The above relation is obtained using the Eq. (13) and the solutions of the resulting self-consistent equations of $\overline{g}_{jj}$; see (37-40). There indeed we find

$$\overline{g}_{11} = \frac{w^*\overline{\gamma}_1 - c\,w/\kappa}{1-c^2},\ \overline{g}_{22} = \frac{w^*\overline{\gamma}_2 - c\,w}{1-c^2}. \tag{65}$$

Solving Eqs. (62,63) for the $\overline{\gamma}_j$'s we get

$$|w|^2\gamma_1 = \frac{-\alpha(1-\kappa) + \sqrt{\alpha^2(1-\kappa)^2 + 4|w|^4}}{2\kappa}, \tag{66}$$

$$|w|^2\gamma_2 = \frac{\alpha(1-\kappa) + \sqrt{\alpha^2(1-\kappa)^2 + 4|w|^4}}{2}. \tag{67}$$

Consequently we derive the Green's function:

$$\overline{\mathsf{g}}_{\mathsf{C}}(z,z^*) = \frac{\alpha(\kappa-1) + \sqrt{\alpha^2(1-\kappa)^2 + 4|z|^2}}{2\alpha\kappa z} - \frac{c}{\kappa\alpha}, \tag{68}$$

where $\alpha = (1-c^2)$. Finally, using the Gauss law (8), for $\kappa \leq 1$, we find

$$\overline{\rho}_{\mathsf{C}}(z,z^*) = \frac{1}{\pi\kappa\alpha\sqrt{\alpha^2(1-\kappa)^2 + 4|z|^2}}. \tag{69}$$

On the other hand, the density is zero outside the ellipse (55). Taking account the $1/z$ terms for $z \to 0$, and the identity $\partial/\partial z^*(1/z) = \delta(z)\delta(z^*)$, we get an additive term $(1-\kappa^{-1})\delta(z)\delta(z^*)$ for $\kappa > 1$. This term is consistent with the observation about the rank of C in Sec. II. For $c = 0$, this result (69) yields spectral density for the uncorrelated case which matches with the result obtained in Ref. [34] if we replace z by $\sqrt{\kappa}\,z$.

In Fig. 7, we compare the radial distribution, $\overline{\rho}_{\mathsf{R}}(r)$, with our theory (69) by integrating the θ variable where $z = r\,\exp(i\theta)$. We consider three different c values as chosen in Fig. 1. For instance in Fig. 7(a) we compare the radial density with the theory (69) for $c = -1/4$. Since the radial density does not depend on the sign of c, in figure (c) we get the same result for $c = 1/4$. The finite-N effect [34] can be seen in the peaks and in the tails of the densities. Similarly in Fig. 8, we compare the marginal density distribution of the real and the imaginary parts of the eigenvalues. The distributions we obtain for the one is by integrating over the other, e.g., the density for the real part, $\overline{\rho}_X(x)$, is obtained by integrating over y from $\overline{\rho}_{X,Y}(x,y) \equiv \overline{\rho}(z,z^*)$. For $c = 0$ both densities are symmetric along both axis. However, for $c \neq 0$, the symmetry along the x-axis is broken. With a simple calculation it can be shown that for $c \to 1$, $\overline{\rho}_X(x)$ converges to the Marčenko Pastur distribution [17] implying thereby that all the real components of the spectra of C are non-negative. As shown in the figure, our theory closely describes these densities except the peaks in $\overline{\rho}_Y(y)$ at $y = 0$, which are in fact a finite-N effect. These peaks are well studied for the Ginibre ensemble [51] where analytical results are known in much detail [52–54].

VII. SUMMARY AND CONCLUSION

To summarize the work, we begin with a few important remarks. In physics, nonsymmetric random matrices have been of importance from different perspectives [13–15]. For the correlation matrices, however, these are important in order to understand time evolution of a multivariate complex system or to understand statistical behaviour of two different statistical systems. Usually, Wishart's approach is used in dressing the noise from an empirical correlation matrix where the spectral analysis is at the cornerstone. Including linear correlations, however, provides a better way of understanding effects of the actual correlations in the spectral statistics. The importance is evident from Refs. [4–7, 18, 55]. However, from the applications point of view, the model we have studied in this paper is open for a detailed treatment. On the other hand, from the theoretical point of view, there are still many problems to solve. One example of these being

the finite-N results, which have been obtained by using the supersymmetric technique for the CWOE [25, 26].

In this paper we have focused mainly on the domain of the bulk of complex eigenvalues under the influence of actual correlations. We have derived analytic result for the contour enclosing the bulk of the eigenvalues for general η for which the full correlation matrix ξ is positive definite. One important finding of this paper is the ellipse which explains the boundary of eigenvalues for a system dominated by autocorrelations of equal strength. Beside that we have shown analytically that such contours depend on the nonsymmetry in the actual correlations. In this paper, results are demonstrated using tridiagonal η matrices, which is a simple case that covers most of the analytic premises and subtleties of the problem. Also we have shown that effects of the nonsymmetry can well be observed in the singular values of η but this interpretation of the nonsymmetry is not so straightforward as we have for the complex eigenvalues.

As far as applications are concerned, there have been growing interests in nonsymmetric correlations, particularly in financial data analysis. Perhaps the closest example is the study of correlations of stock prices with their volume data [56], where the main emphasis has so far been the bi-variate time series [57]. We believe that the generalization to the multi-stock data will shed more light and there our results could be useful. Finally, we believe that our results may not be confined to the multivariate analysis, as can be deduced from the historical developments of RMT [58].

VIII. ACKNOWLEDGMENTS

The authors of this paper are thankful to Thomas H. Seligman and F. Leyvraz for useful discussions and consistent encouragements. Financial support from CONACyT through Project No. 154586 and No. PAPIIT UNAM RR 11311 is acknowledged. Vinayak was supported by DGAPA/UNAM as a postdoctoral fellow.

Appendix A: Inverse

The inverse of matrix we want to calculate may be viewed as

$$\left(\tilde{\mathsf{W}} - \Sigma\right) \equiv \mathsf{M} = \begin{pmatrix} \mathbf{a} & \mathbf{b} \\ \mathbf{c} & \mathbf{d} \end{pmatrix}, \tag{A1}$$

where all the matrices are of dimension $(N+T)\times(N+T)$. Matrices $\mathbf{b}$ and $\mathbf{c}$ are diagonal:

$$\mathbf{b} \;=\; -\begin{pmatrix} \overline{g}_{2\,\overline{2}}\mathbf{1}_N & \mathbf{0} \\ \mathbf{0} & \kappa\overline{g}_{1\,\overline{1}}\mathbf{1}_T \end{pmatrix},\; \mathbf{c} = -\begin{pmatrix} \overline{g}_{\overline{2}\,2}\mathbf{1}_N & \mathbf{0} \\ \mathbf{0} & \kappa\overline{g}_{\overline{1}\,1}\mathbf{1}_T \end{pmatrix}, \tag{A2}$$

and for the diagonal blocks we have

$$\mathbf{a} = \begin{pmatrix} \overline{\mathsf{a}}_1 & \mathbf{0} \\ \mathbf{0} & \overline{\mathsf{a}}_2 \end{pmatrix},\; \mathbf{d} = \begin{pmatrix} \overline{\mathsf{d}}_1 & \mathbf{0} \\ \mathbf{0} & \overline{\mathsf{d}}_2 \end{pmatrix}. \tag{A3}$$

We use Schur components of $\mathbf{a}$ and of $\mathbf{d}$, viz., $\mathbf{d}-\mathbf{c}\mathbf{a}^{-1}\mathbf{b}$ and $\mathbf{a}-\mathbf{b}\mathbf{d}^{-1}\mathbf{c}$, respectively, assuming that none of them are singular. Then the inverse of the matrix [59] we get is

$$\mathsf{M}^{-1} = \begin{pmatrix} \mathsf{S}^{-1} & -\mathsf{S}^{-1}\mathbf{b}\mathbf{d}^{-1} \\ -\mathbf{d}^{-1}\mathbf{c}\mathsf{S}^{-1} & (\mathbf{d}-\mathbf{c}\mathbf{a}^{-1}\mathbf{b})^{-1} \end{pmatrix}, \tag{A4}$$

where $\mathsf{S} = \mathbf{a} - \mathbf{b}\mathbf{d}^{-1}\mathbf{c}$. Thus we get (29)

[1] S. S. Wilks, *Mathematical Statistics* (Wiley, New York, 1962).
[2] R. J. Muirhead, *Aspects of Multivariate Statistical Theory*, Wiley Series in Probability and Statistics (Wiley, 2009).
[3] J. Wishart, Biometrika **20A**, 32 (1928).
[4] L. Laloux, P. Cizeau, J. P. Bouchaud and M. Potters, Phys. Rev. Lett. **83**, 1467 (1999).
[5] V. Plerou, P. Gopikrishnan, B. Rosenow, L. A. N. Amaral and H. E. Stanley, Phys. Rev. Lett. **83**, 1471 (1999).
[6] V. Plerou, P. Gopikrishnan, B. Rosenow, L. A. Nunes Amaral, T. Guhr, and H. E. Stanley, Phys. Rev. E **65** 066126 (2002).
[7] F. Lillo and R. N. Mantegna, Phys. Rev. E **72**, 016219 (2005).
[8] M. C. Münnix, T. Shimada, R. Schäfer, F. Leyvraz, T. H. Seligman, T. Guhr, and H. E. Stanley, Sci. Rep. **2**, 644 (2012).
[9] F. Luo, J. Zhong, Y. Yang and J. Zhou, Phys. Rev. E **73** 031924 (2006).
[10] P. Šeba, Phys. Rev. Lett. **91**, 198104 (2003).
[11] M. S. Santhanam and P. K. Patra, Phys. Rev. E **64**, 016102 (2001).
[12] M. L. Mehta, *Random Matrices* (Academic Press, New York, 2004).
[13] T. A. Brody, J. Flores, J. B. French, P. A. Mello, A. Pandey and S. S. M. Wong, Rev. Mod. Phys. **53**, 385 (1981).
[14] T. Guhr, A. M. Groeling and H. A. Weidenmüller, Phys. Rep. **299**, 189 (1998).
[15] C. W. J. Beenakker, Rev. Mod. Phys. **69**, 731 (1997).
[16] R. R. Müller, IEEE Transactions on Information Theory, **48**, 2495 (2002);
[17] V. A. Marčenko and L. A. Pastur, Math. USSR Sb. **1**, 457 (1967).
[18] Vinayak, R. Schäfer and T. H. Seligman, Phys. Rev. E **88**, 032115 (2013).
[19] J. W. Silverstein, J. Multivariate Anal. **55**, 331 (1995).
[20] A. M. Sengupta and P. P. Mitra, Phys. Rev. E **60**, 3389 (1999).

[21] Z. Burda, J. Jurkiewicz and B. Waclaw, Phys. Rev. E **71**, 026111 (2005).

[22] S. H. Simon and A. L. Moustakas, Phys. Rev. E **69**, 065101(R) (2004).

[23] J. Baik *et al. Ann. Probab.* **33** 1643 (2005) ; S. Péché *J. Multivariate Anal.* **97**, 874 (2006).

[24] Vinayak and A. Pandey, Phys. Rev. E **81**, 036202 (2010).

[25] C. Recher, M. Kieburg, and T. Guhr, Phys. Rev. Lett. **105**, 244101 (2010).

[26] C. Recher, M. Kieburg, T. Guhr and M. R. Zirnbauer, J. Stat. Phys. **148**, 981 (2012).

[27] I. M. Johnstone, Ann. Statist. **29**, 295 (2001).

[28] C. Biely and S. Thurner, Quant. Financ. **8**, 705 (2008).

[29] J.-P. Bouchaud, L. Laloux, M. A. Miceli and M. Potters, Eur. Phys. J. **55**, 201 (2007).

[30] J. P. Bouchaud and M. Potters, arXiv:0910.1205v1 **q-fin.ST**, (2009).

[31] D. Wang, B. Podobnik, D. Horvatić and H. E. Stanley, Phys. Rev. E **83**, 046121 (2011).

[32] G. Livan and L. Rebecchi, Eur. Phys. J. B **85**, 213 (2012).

[33] Vinayak, Phys. Rev. E **88**, 042130 (2013).

[34] Z. Burda, A. Jarosz, G. Livan, M. A. Nowak and A. Swiech, Phys. Rev. E **82**, 061114 (2010).

[35] S. Orourke and A. Soshnikov, arXiv:1012.4497 [math.PR].

[36] F. Götze, A. Tikhomirov, arXiv:1012.2710v1 [math.PR].

[37] J. R. Ipsen and M. Kieburg, Phys. Rev. E **89**, 032106 (2014).

[38] R. R. Müller, Acta Phys. Pol. B **36**, 1001 (2005).

[39] G. Akemann, J. R. Ipsen and M. Kieburg, Phys. Rev. E **88**, 052118 (2013).

[40] G. Akemann , M. J. Phillips and H-J. Sommers, J. Phys. A: Math. Theor. **43** 085211 (2010).

[41] H.-J. Sommers, A. Crisanti, H. Sompolinsky, and Y. Stein, Phys. Rev. Lett. **60**, 1895 (1988).

[42] E. Gudowska–Nowak, R. A. Janik, J. Jurkiewicz and M. A. Nowak, Nucl. Phys. B **670**, 479 (2003).

[43] J. Feinberg and A. Zee, Nuclear Physics B **504**, 579 (1997).

[44] R. A. Janik, M. A. Nowak, G. Papp, J. Wambach, and I. Zahed, Phys. Rev. E **55**, 4100 (1997); R. A. Janik, M. A. Nowak, G. Papp, and I. Zahed, Nucl. Phys. B **501**, 603 (1997).

[45] Z. Burda, R. A. Janik, and B. Waclaw, Phys. Rev. E **81**, 041132 (2010).

[46] E. Brezin, C. Itzykson, G. Parisi and J.-B. Zuber, Commun. Math. Phys. **59**, 35 (1978).

[47] A. Pandey, Ann. Phys. (N.Y.) **134**, 110 (1981).

[48] D. Kulkarni, D. Schmidt and Sze-Kai Tsui, Linear Algebra and its Applications **297**, 63 (1999).

[49] It is understood that in both cases the bulk density is normalized to $1 - N^{-1}$.

[50] Vinayak and M. Žnidarič, J. Phys. A: Math. Theor. **45**, 125204 (2012).

[51] J. Ginibre, J. Math. Phys. (N.Y.) **6**, 440 (1965).

[52] E Kanzieper and G. Akemann, Phys. Rev. Lett. **95**, 230201 (2005).

[53] P. J. Forrester and T. Nagao, Phys. Rev. Lett. **99**, 050603 (2007).

[54] A. Edelman and N. R. Rao, Acta Numerica **14**, 233 (2005)

[55] T. Wirtz and T. Guhr, Phys. Rev. Lett. **111**, 094101 (2013).

[56] K Karpio , P. Łukasiewicz and A. Orlowski, Acta. Phys. Polonica A **121**, b61 (2010).

[57] B. Podobnik and H. E. Stanley, Phys. Rev. Lett. **100**, 084102 (2008).

[58] N. C. Snaith, P. J. Forrester, J. J. M. Verbaarschot, J. Phys. A **36**, R1-R10, 2859 (2004).

[59] D. S. Bernstein *Matrix Mathematics: Theory, Facts and Formulas*, (Princeton University Press, 2005).